

Molecular dynamics simulation of synchronization in driven particles

Tiare Guerrero* and Danielle McDermott†

Department of Physics, Pacific University, Forest Grove, OR 97116

(Dated: December 28, 2020)

Particles driven across a washboard potential energy landscape exhibit a variety of synchronization effects in experimental systems including magnetically driven colloidal particles confined by light-fields. We discuss a simple numerical model that provides insight to synchronization behavior using molecular dynamics simulations for particles moving through a viscous liquid. We demonstrate how to visualize the system with numerical representations of the landscape and animations of the particle motion. Our results show a variety of systems that synchronize particle velocity as a function of applied driving force, and characterize these behaviors with force-velocity curves and phase diagrams. We include sample code and exercises for students with opportunities to reproduce our results and propose new numerical experiments.

I. INTRODUCTION

Synchronization is a universal phenomena in which individual oscillators adjust frequency due to interaction or an external stimulus [1]. Synchronous behaviors where oscillators move in-phase (i.e. in time) are observed in many everyday systems such as the flickering candle flames coupled by temperature fluctuations [3], vibrations of singing wineglasses [4], and metronomes coupled through a supporting platform [5]. Biological systems benefit from cooperative synchronization such as birds coordinating wing flaps to optimize energy use during flight [6], frogs alternating croaking patterns [7], and humans synchronizing clapping in time with music [8]. At a cellular level, neurons simultaneously fire in cardiac muscle [9] and brain tissue [10].

A particular form of synchronization is phase-locking or mode-locking, which first appeared in the scientific literature with Huygens' 1665 experiments on the motions of two wall-mounted pendulum clocks. Huygens demonstrated the tendency of the pendula to swing in time due to interactions through the wall, no matter the original phase of the clocks [2]. Dynamical systems exhibit phase-locking when oscillators with different rhythms couple so the frequency ratio or mode is an integer number [12]. The phenomena is often studied with simplified computational models and can be visualized with phase plots or Lissajous figures. A mode-locked system is confined to a closed loop in a parametric space showing the relationship between two periodic functions with patterns determined by the mode, first reported in 1857 [13] and easily generated with a computer code or oscilloscope [14]. (*As we will demonstrate in phase plots in Figs. X, Y, Z*)

External forcing can cause or regulate synchronization. For instance a pacemaker (an electrical generator) pulses to regulate a heart beat or controlling the pattern of flashing fireflies with a pulsed light [15]. These behaviors

can be modeled with numerical studies where a driving force is applied to simple harmonic system, either coupled oscillators or a single particle driven across a periodic potential landscape. A single particle oscillator within a potential well is much like a skateboarder in a half-pipe or a child on a swing moving back and forth through equilibrium. Single particle studies are useful to understand synchronization in the absence of collective effects. With a constant or dc drive the landscape modulates the particle velocity, below some threshold below the dc force is not strong enough to push the particle across a potential maximum so the average velocity is zero, a phenomena known as depinning [23], and dissipating energy from the system at all driving forces. A sinusoidal or ac drive creates mode-locking, where the average particle velocity is fixed for a range of dc drive forces [24].

Dynamical mode-locking is observed in quantum electronic devices such as Josephson junctions [16, 17]. A single junction contains two superconducting layers which sandwich an insulating layer. When subject to an external voltage, Cooper pairs in the superconducting materials tunnel through the insulating layer. Phase-locking is observed as stepped regions in current-voltage (I-V) relationship in these devices, where voltage is the analog of external driving force and current is that of particle velocity. Known as Shapiro steps, these phase locked currents have been observed due to applied ac voltages in single Josephson junctions [19, 21] and coupled arrays of junctions [20]. Shapiro steps vary in width depending on the strength of the applied AC forces, and are observed in a variety of systems displaying non-Ohmic behavior in voltage-current curves, including ac and dc driven charge and spin density waves.

II. COLLOIDAL MODELS

Experiments with colloid particles, such as plastic beads suspended in highly de-ionized water [], are useful model systems to understand complex behaviors. Experiments of colloid particles confined in optical traps subject to external driving forces have been used to examine

*Electronic address: guer9330@pacificu.edu

†Electronic address: mcdermott@pacificu.edu

the microscopic dynamics of individual particles during mode-locking, which cannot be easily imaged in electronics. Colloidal particles trapped in light fields are a useful medium for studying complex dynamical behaviors due to their relatively large size of microns, making them relatively simple to control and image. Additionally colloids can mimic different systems since the interaction forces between colloids can be modified by tuning the chemistry of the suspending fluid or surface ligands of the particles. Because colloids are easy to control and study, they are used as experimental models for systems relatively hard to access and visualize, such as cold atoms or electron gases [29]. Mode-locking in colloids has been achieved in systems interacting via magnetic dipoles or electric forces in experiment [25, 30] and simulation [27, 28].

Here we perform numerical studies on the synchronized dynamics of confined particles driven over a washboard shaped potential energy landscape. We chose this model for its relevance to condensed matter systems and ease of simulation. Numerical modeling of colloids can provide mechanistic insight that can be difficult to achieve in experimental conditions where Brownian motion and other sources of noise dominate. The period of the substrate can be used to control the intrinsic velocity of the dc driven particle, and the applied ac drive can create Shapiro steps in the force-velocity relationship.

We describe our molecular dynamics model in Section III. In this section, we restrict our discussion to a single particle, and include additional information for multiple particles in Section IV B. We summarize our results in Section IV including synchronized motion of a single confined particle driven across a periodic landscape in Section IV A and multiple interacting particles in Section IV B, including stationary propagation of high density kinks in Sec. IV C. We include code to simulate and visualize the landscape and dynamics in this section and supplementary material. We present these results using standard tools of non-linear oscillators such phase diagrams of velocity versus position. In each section we suggest exercises for interested students, as summarized in Section VII.

III. MOLECULAR DYNAMICS SIMULATION

In this section we describe the dynamics of the particles using the model forces and the motion using an modified form of Newton's second law suitable for microscopic particles in a suspending fluid.

We use a classical two-dimensional model for studying the dynamics of N interacting particles. Particles are confined in a two-dimensional (2D) simulation of area $A = L \times L$ where $L = 36.5a_0$ where a_0 is a dimensionless unit of length. An individual particle i has position $\vec{r}_i = x_i\hat{x} + y_i\hat{y}$ and velocity $\vec{v}_i = d\vec{r}_i/dt$. Particles are subject to periodic boundary conditions such that a particle leaving the edge of the system is mapped back to a position within the simulation by the transformation

$$x_i + L \rightarrow x_i \text{ and } y_i + L \rightarrow y_i.$$

Particles are subject an external time-dependent driving force $\vec{F}_D(t)$ applied parallel to the y -direction. We model this force as

$$\vec{F}^D(t) = [F^{DC} + F^{AC} \sin(\omega t)]\hat{y}, \quad (1)$$

with modifiable parameters including a constant component F^{DC} , and a time dependent component with amplitude F^{AC} and frequency $\omega = 2\pi f$. When F^{DC} is non-zero, we slowly increase F^{DC} from zero to avoid transient effects.

We confine the particles using a position dependent potential energy function, called a landscape or substrate. The confining force is calculated as $\vec{F}_i^l(\vec{r}_i) = -\nabla U_i(\vec{r}_i)$. The periodic landscape is modulated in the y -direction as

$$U_{washboard}(y) = U_0 \cos(N_p \pi y / L) \quad (2)$$

where N_p are the number of periods, and U_0 is an adjustable parameter to set the depth of the troughs. We define the substrate strength to be the force $A_p = 2\pi U_0 / L$.

We model the particle dynamics with an overdamped equation of motion. The term ‘‘overdamped’’ or critically damped indicates that an oscillator cannot undergo periodic undulations due to some external force. In our colloidal model we assume the damping comes from the viscosity of the fluid, where a sphere of radius $0.5\mu\text{m}$ has a Reynolds number of $R \approx 10^{-6}$, indicating that linear drag dominates its motion. See Section VII Exercise 1 for more information about the Reynold's number. We model this nonconservative force, with the linear friction $\vec{F}_{drag} = -\eta\vec{v}_i$ sufficient so that the acceleration of the particle is zero. Such a model is appropriate when the particles are small and the viscosity of the suspending medium is high. This model should be familiar to readers modeling Millikan's oil drops in a standard classical mechanics text [35].

Newton's second law for an individual particle $m\vec{a}_i = \sum \vec{F}$ is simplified by the assumption \vec{a}_i is zero in overdamped model. The equation of motion for an isolated particle

$$\eta\vec{v}_i = \vec{F}_i^l + \vec{F}^D(t). \quad (3)$$

where the viscosity coefficient $\eta = 1$. In Section VII Exercise 2 we invite the reader to confirm this result. The equation of motion provides a direct calculation of the velocity of an individual particle from its location \vec{r}_i with respect to other particles j .

The molecular dynamics simulation is controlled by a `for()` loop which runs from an initial to maximum integer number of time steps t_i . Each integer time step interval $t_{i+1} - t_i$ represents a simulation time interval of Δt simulation units. At each time step we evaluate the net force on each particle as a function of its position $\vec{r}_i(t)$ and then integrate the equation of motion to move

particles to an updated position $\vec{r}_i(t + \Delta t)$. Since the acceleration is zero, [more background here - do the students necessarily know the Verlet method? no] the Verlet method simplifies to the Euler method, which is used to calculate the position at subsequent time steps.

$$\vec{r}_i(t + \Delta t) = \vec{v}_i(t)\Delta t + \vec{r}_i(t). \quad (4)$$

The units of the simulated variables are summarized in Table I.

TABLE I: Simulation units.

| Quantity | Unit |
|------------------------------------|---|
| length | a_0 |
| energy | $E_0 = q^2 Z^{*2} / 4\pi\epsilon\epsilon_0 a_0$ |
| dimensionless interaction strength | q |
| effective colloidal charge | Z^* |
| solvent dielectric constant | $\epsilon\epsilon_0$ |
| force | E_0/a_0 |
| viscosity/damping constant | η |
| time | η/E_0 |
| velocity | $E_0/\eta a_0$ |

IV. RESULTS

We demonstrate how a single particle (Sec. IV A) and many particles move (Sec. IV B) in response to this applied force in a variety of environments. In Sec. IV C we set F^{DC} to zero and track the motion of a high density area of a particle chain (i.e. kink dynamics).

A. Single particle system

We drive a single particle across a periodic landscape along the y-direction

$$U_l(y) = U_{0y} \cos(N_p \pi y / L) \quad (5)$$

with $N_p = 20$ troughs in the landscape and landscape period $\lambda = L/N_p = 1.825a_0$. This is illustrated in Fig. 2(a) where the red (blue) regions show local maxima (minima). The code for generating a two dimensional colored plot of the potential landscape is calculated by evaluating the analytic function in Eq. ?? for a grid of values (x_n, y_n) . The numerical implementation of the landscape is calculated with

$$F_y(y) = A_p \sin(N_p \pi y / L) \quad (6)$$

where $A_p = 0.1$.

Because we are performing molecular dynamics for a single particle on a smooth potential energy landscape, we use a large simulation time step of $\Delta t = 0.01$. In

Sec. IV B, we decrease the time step to treat multiple particle interactions.

We drive the particle with $F^{AC} = 0.2$, $F^{DC} = 0.01$, and $f = 0.01$ cycles per time unit. When the superposition of F^{AC} and F^{DC} is large enough to overcome the barrier height of the landscape troughs, the particle hops between troughs in the energy landscape. In Fig. 1 we show the relationship between the applied force and particle position. In Fig. 1(a) we plot the applied driving force as a function of time and in Fig. 1(b) we show the position of the particle as a function of time. The initial position is near $y = 0$ and the initial driving force is minimum $F_D(t = 0) = F^{DC}$. Over the time period $T/2 = 50$ the particle moves in the positive y-direction while $F_D(t) > 0$ through three substrate troughs, reaching a maximum of $y/\lambda = 3$. When $F_D(t) < 0$ the particle moves in the negative y-direction reaching a minimum position of $y/\lambda = 1$ over the period $T = 1/f = 100$. The average velocity \bar{v}_y is the average displacement $\Delta y = y(t_0 + T) - y(t_0)$ over the period of the driving force. In Fig. 1 the average displacement during one time period is a single wavelength of the substrate $y(t_0 + T) - y(t_0) = \lambda$. Thus the average velocity is $\bar{v}_y = \lambda f$.

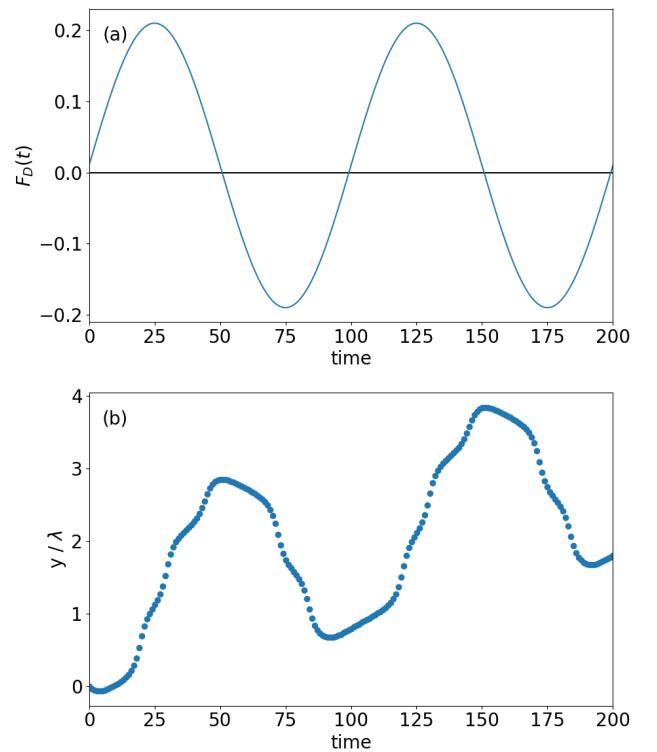


FIG. 1: The position as a function of time of a single driven particle normalized by the period of the substrate λ .

Phase locked steps occur for average displacements in integer multiples of the substrate period $n\lambda$.

We sample the average velocity $\langle v_y \rangle$ as a function of F^{DC} .

The hopping pattern of the driven particle is periodic, and could be achieved over a range of F^{DC} . We explore the ranges of periodic hopping patterns by increasing F^{DC} as a function of time, as shown in Fig. 2. We apply an external applied force, with a constant F^{AC} with frequency $\omega = 2\pi f$ then slowly increase F^{DC} at a rate of $\Delta F^{DC} = 0.001$ every $\Delta t = 4000$ integer timesteps or 40 time units. By modifying F^{DC} we achieve a variety of oscillation modes. A mode is a periodic pattern of hops with a constant average particle velocity, \bar{v}_y over a range of driving forces F^{DC} . We illustrate mode-locking in the velocity-force plot in Fig. 2(b). Here \bar{v}_y is increasing in non-uniform steps, with a quantized height of $\bar{v}_y = n\lambda f$, where n is an integer, $\lambda = L/N_p = 36.5/20 = 1.825$ is the spatial period, or wavelength of the landscape, and $f = 0.01$ cycles per time unit.

Our simulations reproduce results presented in Juniper *et al.* [25, 26] which demonstrated mode locking in experiments of driven colloids on a optical periodic landscape.

We illustrate the hopping pattern in Fig. 2(b) and show the dynamics in supplementary materials [36].

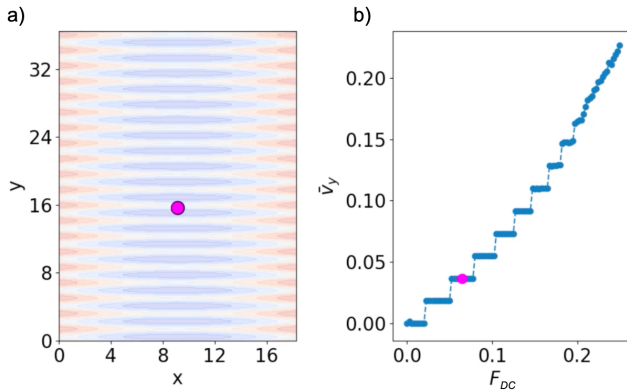


FIG. 2: **(a)** The particle is driven with a constant amplitude F^{AC} and frequency ω through a periodic spatial potential landscape. The landscape is represented with a colormap where blue are minima and red are maxima in the potential. **(b)** An average particle velocity in the y-direction \bar{v}_y as a function of a constant driving force F^{DC} . In the animation available in Ref. [36] the magenta dot represents the average velocity of the particle \bar{v}_y at which the particle in Fig. 1(a) is moving.

B. Synchronization in multi-particle systems

Particles in confined geometries behave differently than free particles. Stabilized charged particles form patterns due to the interplay of the confining landscape and particle interactions. Narrow channels studies are useful to provide insights of how particles move through systems

such as charge carries in quantum wires [31] and slime molds in microchannels [32]. In multi-particle simulations, we confine the particles to a narrow region along the x -direction using a periodic function

$$U_{q1D}(x) = U_{q0} \cos(\pi x/L) \quad (7)$$

where U_{q0} defines the channel depth. This quasi-one-dimensional geometry confines the particles primarily to move along the y -direction but allows for some lateral motion of particles. Otherwise the repulsive interaction between particles would cause them to spread throughout the system. The total landscape potential energy function is the sum

$$U_{landscape}(x, y) = U_{q1D}(x) + U_{washboard}(y) \quad (8)$$

We explore collective effects in a twenty particle system confined to a narrow channel, as shown in Fig. 2(a). We create the confining channel with a sinusoidal function with a single period.

$$U_l(x) = U_{0x} \cos(\pi x/L). \quad (9)$$

The landscape potential energy is illustrated in Fig. 3(a) where red regions are high potential and blue regions are low potential.

We model particle interaction forces $\vec{F}_{ij} = -\nabla U_{ij}(r_{ij})$ with the Yukawa potential energy

$$U_{ij}(r_{ij}) = \frac{E_0}{r_{ij}} e^{-\kappa r_{ij}}, \quad (10)$$

where particle i and j are distance $r_{ij} = |\vec{r}_i - \vec{r}_j|$ apart. This screened Coulomb potential is scaled in terms of energy unit E_0 defined in Table I. $\kappa = 1/R_0$ is the screening parameter that describes the length scale at which particles interact. We fix the screening length scale R_0 to be a_0 (i.e. unity in simulation units). In experiments charge screening is observed due to ions in the suspending fluid and the charges of surrounding particles which reduces the interaction range of individual particles. Because the particles interact over short ranges, the numerical models can be run efficiently using a neighbor list algorithm determined using a cell method. [explain and reference!]

Newton's second law can be rearranged to the equation of motion a single particle subject to collective effects is

$$\eta \vec{v}_i = \vec{F}_i^l + \sum_{i \neq j}^N \vec{F}_{ij} + \vec{F}_D(t). \quad (11)$$

The initial configuration of the system is shown in Fig. 3(a). We annealed the system into a ground-state configuration by raising the system to a high temperature T , and slowly lowering the temperature in steps of $dT = -0.01$ until the particles form a buckled chain in the low region of the channel due to the competition between particle repulsion and channel confinement. The

interparticle forces between neighboring particles cause the system to form a buckled chain. The molecular dynamics of simulated annealing is described in Ref. ???. Once the ground state particle configuration is obtained, no further annealing is necessary, so the our simulations begin with particle configurations that result from the annealing process, as listed in Appendix [ref] and available in supplementary material.

When a single particle is driven, the neighboring particles act similarly to a periodic landscape to impede its motion. A driven particle can exhibit mode locking with a well-chosen AC drive and frequency. In the attached movie, Figure2.mp4, we show the complex dynamics of mode locking, where the driven particle leap-frogs past the other particles.

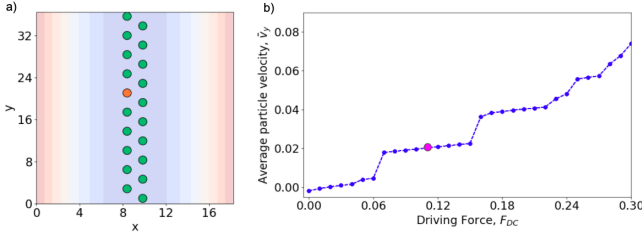


FIG. 3: **(a)** A single particle (colored orange - mark in some manner for non-color views) is driven with a constant amplitude F^{AC} and frequency ω through 19 neighboring particles (colored green - mark differently) confined by a quasi one-dimensional channel. The landscape is colored as in Fig. ??(a). **(b)** Average \bar{v}_y versus F^{DC} , where \bar{v}_y is the average particle velocity of the driven particle in the y-direction.

C. Kinked system

We confine N particles to $N - 1$ troughs to create a local high density region. $F^{DC}/F^{AC} = 1$ [CHECK!]

V. QUASI-PERIODIC SUBSTRATE

VI. CHAOTIC DYNAMICS

VII. ASSOCIATED PROBLEMS

1. Stokes' law the viscous drag on a sphere is $\vec{F}_{lin} = 3\pi\eta D\vec{v}$ where the fluid viscosity is η , D is the particle diameter. Assuming a colloid with diameter $D = 1\mu m$ and the viscosity of water at room temperature is $\eta = 0.01cm^2/sec$ Reynold's number $R = Dv\rho/\eta$ where ρ is the fluid density and v the particle's speed. When R is small, the quadratic and higher order drag terms may be ignored in favor of the linear drag term. A typical v in experi-

ment is on the order of $v \sim 1\mu/s$, thus $R \approx 10^{-6}$.

2. Newton's second law states that the sum of forces on a particle is proportional to the acceleration of the particle.

$$m\vec{a}_i = \sum \vec{F} \quad (12)$$

Demonstrate that Eq. 11 is obtained from Newton's second law.

3. Kuramoto model = overdamped interacting rotors/oscillators are used to model coupled oscillator systems - no substrate or external drive so far as I can see - this seems baked into the oscillator properties/interactions
4. Brownian motion without fluid dynamics using Ermak's algorithm
5. Frenkel-Kontorova and competing length scales for low temperature systems where thermal fluctuations are negligible
6. The Fokker-Planck Equation
7. Aubrey-Kontorova + commensurability
8. nanotribology
kink motion Vanossi et al J.Phys.: Condens. Matter 19 (2007)

VIII. CONCLUSION

IX. SUPPLEMENTARY MATERIALS

A. Grid Contour Plot of landscape

Testing section - how will putting the code directly in the appendix appear?

```
#####
#ADD CONTOUR PLOT
#####
def add_contour(ax,L,N,corrugated = True):
    '''
    Hardwired to color quasi1D potential
    that contains
    the particles in a trough.
    Can add the washboard/corrugated substrate.

    Required Arguments

    Optional Arguments:

    corrugated (default = True)
    Adds the washboard in the y-direction.
    Hardwired for a single parameter set.
```

'''

a_p = L/N

```
#we don't want to cover the entire range
X = np.arange(0, L/2.0, 0.1)
Y = np.arange(0, L, 0.1)
X, Y = np.meshgrid(X, Y)
```

```
Z_mag = 2.0 # set by what "looks good"
Z = Z_mag*np.sin(2*np.pi*X/L)
if corrugated == True:
    Z += np.sin(2*np.pi*(Y+1.75)/a_p)
```

cmap=cm.coolwarm_r

```
#alpha = transparency. set by what looks good.
cset = ax.contourf(X,Y,Z,cmap=cmap,alpha=0.25)
```

```
#ax1.set_xlim(15,20)
#ax1.set_ylim(15,20)
```

```
#ax1.set_xlabel(r"$X$")
#ax1.set_ylabel(r"$y$",rotation='horizontal',ha='right')

#ax1.set_xticks([])
#ax1.set_yticks([])
return
```

Acknowledgments

We acknowledge Harvey Gould and Jan Tobochnik, who invited us to write the article and supported its development. Charles and Cynthia Reichhardt advised the project and provided the original molecular dynamics code written in the C programming language. We acknowledge funding from the M.J. Murdock Charitable Trust and the Pacific Research Institute for Science and Mathematics (PRISM).

-
- [1] A. Pikovsky, M. Rosenblum, and J. Kurths, *Synchronization: A Universal Concept in Nonlinear Sciences* (Cambridge Univ. Press, Cambridge, 2003).
 - [2] M. Bennett, M.F. Schatz, H. Rockwood, and K. Wiesenfeld, Huygens' clocks, *Proc. Roy. Soc. A* **458**, 563 (2002).
 - [3] K. Okamoto, A. Kijima, Y. Umeno, and H. Shima. Synchronization in flickering of three-coupled candle flames. *Sci Rep* **6**, 36145 (2016)
 - [4] T. Arane, A. K. R. Musalem and M. Fridman, Coupling between two singing wineglasses, *Am. J. Phys.* **77**, 1066 (2009).
 - [5] J. Jia, Z. Song, W. Liu, J. Kurths, and Xiao, J. Experimental study of the triplet synchronization of coupled nonidentical mechanical metronomes. *Sci. Rep.* **5**, 17008 (2015).
 - [6] S. Portugal, T. Hubel, J. Fritz, S. Heese, D. Trobe, B. Voelkl, S. Hailes, A. M. Wilson and J. R. Usherwood. Upwash exploitation and downwash avoidance by flap phasing in ibis formation flight. *Nature* **505**, 399 (2014).
 - [7] I. Aihara, T. Mizumoto, T. Otsuka, H. Awano, K. Nagira, H. G. Okuno and K. Aihara. Spatio-Temporal Dynamics in Collective Frog Choruses Examined by Mathematical Modeling and Field Observations. *Sci Rep* **4**, 3891 (2014).
 - [8] P. Tranchant, D. T. Vuvan, and I. Peretz, Keeping the Beat: A Large Sample Study of Bouncing and Clapping to Music. *PLoS ONE* **11**(7): e0160178. (2016).
 - [9] G. Martin Hall, Sonya Bahar, and Daniel J. Gauthier, Prevalence of Rate-Dependent Behaviors in Cardiac Muscle. *Phys. Rev. Lett.* **82**, 2995 (1999).
 - [10] W. Singer. Striving for coherence. *Nature*, **397** 391, 1999.
 - [11] Dutta, S., Parihar, A., Khanna, A. et al. Programmable coupled oscillators for synchronized locomotion. *Nat Commun* **10**, 3299 (2019).
 - [12] P. Bak. The Devil's Staircase. *Physics Today* **39**, 12, 38 (1986).
 - [13] J. A. Lissajous. "Mmoire sur l'Etude optique des mouvements vibratoires," *Annales de chimie et de physique*, 3rd series, 51 (1857) 147-232
 - [14] E. Y. C. Tong, Lissajous figures, *The Physics Teacher* **35**, 491 (1997).
 - [15] D. K. Agrawal, J. Woodhouse, and A. A. Seshia, *Physical Review Letters* **111**, 084101 (2013).
 - [16] B. D. Josephson, *Phys. Letters* **16**, 25 (1962).
 - [17] B. D. Josephson, *Advan. Phys.* **14**, 419 (1965).
 - [18] W. C. Stewart CURRENT-VOLTAGE CHARACTERISTICS OF JOSEPHSON JUNCTIONS *Appl. Phys. Lett.* **12**, 277 (1968).
 - [19] S. Shapiro, Josephson currents in superconducting tunneling: the effect of microwaves and other observations, *Phys. Rev. Lett.* **11**, 80 (1963).
 - [20] S. P. Benz, M. S. Rzchowski, M. Tinkham, and C. J. Lobb, Fractional giant Shapiro steps and spatially correlated phase motion in 2D Josephson arrays, *Phys. Rev. Lett.* **64**, 693 (1990); D. Dominguez and J. V. Jose, Giant Shapiro steps with screening currents, *Phys. Rev. Lett.* **69**, 514 (1992).
 - [21] A. A. Golubov, M. Yu. Kupriyanov, and E. Il'ichev. The current-phase relation in Josephson junctions, *Rev. Mod. Phys.* **76**, 411 (2004).
quote: Phase engineering techniques are used to control the dynamics of long-bosonic Josephson-junction arrays built by linearly coupling Bose-Einstein condensates.
 - [22] Dengling Zhang, Haibo Qiu, and Antonio Muñoz Mateo, Unlocked-relative-phase states in arrays of Bose-Einstein condensates, *Phys. Rev. A* **101**, 063623 (2020).
 - [23] C. Reichhardt and C. J. Olson Reichhardt, Depinning and nonequilibrium dynamic phases of particle assemblies driven over random and ordered substrates: a review, *Rep. Prog. Phys.* **80**, 026501 (2017).
 - [24] C. Reichhardt, and C. J. O. Reichhardt, Shapiro steps for skyrmion motion on a washboard potential with longitudinal and transverse ac drives. *Phys. Rev. B* **92**, (22). (2015).
 - [25] M. P. N. Juniper, A. V. Straube, R. Besseling, D. G. A.

- L. Aarts, and R. P. A. Dullens, Microscopic dynamics of synchronization in driven colloids. *Nat. Commun.* **6**, 7187 (2015).
- [26] Juniper, M. P. N., Zimmermann, U., Straube, A. V., Besseling, R., Aarts, D. G. A. L., Lwen, H., and Dullens, R. P. A. Dynamic mode locking in a driven colloidal system: Experiments and theory. *New Journal of Physics*, **19**(1). (2017).
- [27] S. Herrera-Velarde and R. Castaeda-Priego, Superparamagnetic colloids confined in narrow corrugated substrates, *Phys. Rev. E* **77**, 041407 (2008).
- [28] S. Herrera-Velarde and R. Castaeda-Priego, *J. Phys.: Condens. Matter* **19**, 226215 (2007).
- [29] D. G. Grier, A revolution in optical manipulation. *Nature* **424**, 810 (2003).
- [30] C. Lutz, M. Kollmann, and C. Bechinger, *Phys. Rev. Lett.* **93**, 026001 (2004); C. Lutz, M. Kollmann, C. Bechinger, and P. Leiderer, *J. Phys.: Condens. Matter* **16**, S4075 (2004).
- [31] S. Tarucha, T. Honda, T. Saku, *Solid State Commun.* **1995**, 94, 413.
- [32] A. Gholami, O. Steinbock, V. Zykov, and E. Bodenschatz, Flow-Driven Waves and Phase-Locked Self-Organization in Quasi-One-Dimensional Colonies of *Dictyostelium discoideum*, *Phys. Rev. Lett.* **114**, 018103 (2015).
- [33] D. Frenkel and B. Smit, *Understanding Molecular Simulation: From Algorithms to Applications* (Academic Press, London, 2001).
- [34] M. P. Allen and D. J. Tildesley, *Computer Simulation of Liquids*. Second Edition. Oxford University Press (2017).
- [35] J. Taylor, *Classical mechanics*. University Science Books (2005).
- [36] See Figure1.mp4 in appropriate